




Structure and petrography of the southwestern margin of the Biella pluton, Western Alps

Davide Zanoni


To cite this article: Davide Zanoni (2016) Structure and petrography of the southwestern margin of the Biella pluton, Western Alps, Journal of Maps, 12:3, 597-620, DOI: [10.1080/17445647.2015.1056259](https://doi.org/10.1080/17445647.2015.1056259)



To link to this article: <http://dx.doi.org/10.1080/17445647.2015.1056259>

 View supplementary material 

 Published online: 22 Jun 2015.

 Submit your article to this journal 

 Article views: 33

 View related articles 

 View Crossmark data 

SCIENCE

Structure and petrography of the southwestern margin of the Biella pluton, Western Alps

Davide Zanoni*

Dipartimento di Scienze della Terra "A. Desio", Università degli Studi di Milano, via Mangiagalli, 34, 20133 Milano, Italy

(Received 14 August 2014; resubmitted 21 May 2015; accepted 26 May 2015)

This work presents a new form surface map of the southwestern margin of the Biella pluton at the scale 1:10,000. The Biella pluton is part of the Periadriatic intrusives of the Alps and is emplaced in the continental Sesia-Lanzo Zone of the western Austroalpine domain. The country rocks consist of metapelites and different metagranitoids. Pre-intrusive HP (high pressure) mineral assemblages are dominant in country rocks with the exception of metagranitoids dominated by HT (high temperature) assemblages. The plutonic rocks consist of monzonite with minor syenite. The ductile polyphasic deformation of the country rocks predates the pluton emplacement, with the exception of syn-intrusive folding and shearing, which were recorded in the country rocks of the deeper part of the pluton. Syn-intrusive deformation may be represented by brittle structures that bear mineralisation; however, the majority of the brittle deformation postdates the final emplacement of the pluton. The orientation of the pervasive foliation in the country rocks controls the space available for magma intrusion and possible magmatic flow during emplacement. The inferred diffusion of the thermal aureole in the country rocks is based on the variation in contact metamorphic minerals, which is described by microscopic analysis. The extent of the aureole appears to be controlled by the type of dominant mineral assemblages, rock permeability, and the orientation of the regional foliation in country rocks with respect to the pluton margin. The multiscale structural analysis reveals that the Biella pluton emplaced at a depth as shallow as the greenschist facies conditions or shallower.

Keywords: Periadriatic magmatism; Sesia-Lanzo Zone; intrusion mechanism; contact metamorphism; foliation trajectory map

1. Introduction

Structural and petrographic maps comprise an indispensable data repository for unravelling the tectonic and metamorphic history of crystalline basements. This work presents a 1:10,000 scale form surface map of the southwestern margin of the Biella pluton and its country rocks, similar to maps that encompass the northeastern margins of the Biella and Traversella plutons (Zanoni, 2010; Zanoni, Bado, Spalla, Zucali, & Gosso, 2008). The map represents the finite deformation by reported trajectories of tectonic and magmatic structures and their overprinting relationships with detailed petrographic descriptions of plutonic and country rocks. This type

*Email: davide.zanoni@unimi.it



of representation facilitates the visualisation of the variation of the thermal effect due to pluton emplacement throughout the contact aureole. In the case of intrusive magmatism, this type of map is a useful data reference to infer the mechanism and crustal level of emplacement. The same data can provide insights into the constraints on aureole diffusion in country rocks during the transfer of the latent heat of crystallisation.

2. Geological background

During mature Alpine collision in the Oligocene, the breakoff of the subducted European lithospheric slab induced the production and emplacement of calc-alkaline magmas (Davies & Von Blanckenburg, 1995; Von Blanckenburg & Davies, 1995). These magmas rose along the Periadriatic line, which is the main Alpine crustal break (Figure 1 (a)), and subsequently emplaced in the form of plutons, dykes, and volcanites (Berger, Thomsen, Ovtcharova, Kapferer, & Mergolli, 2012; Bernardelli, Castelli, & Rossetti, 2000; Bigioggero, Colombo, Del Moro, Gregnanin, Macera, & Tunesi, 1994; Callegari, Cigolini, Medeot, & D’Antonio, 2004; Carraro & Ferrara, 1968; Dolenc, 1994; Fodor et al., 2008; Kapferer, Mergolli, Berger, Ovtcharova, & Fügenschuh, 2012; Mayer, Cortiana, Dal Piaz, Deloule, De Pieri, & Jobstraibizer, 2003; Müller, Mancktelow, & Meier, 2000; Oberli, Meier, Berger, Rosenberg, & Gieré, 2004; Pamić & Palincaš, 2000; Romer, Schärer, & Steck, 1996; Romer & Siegesmund, 2003; Rosenberg, 2004; Rossetti, Agangi, Castelli, Padoan, & Ruffini, 2007; Stipp, Fügenschuh, Gromet, Stünitz, & Schmid, 2004; Van Marke de Lummen & Vander Auwera, 1990; Von Blanckenburg, Früh-Green, Diethelm, & Stille, 1992; Von Blanckenburg et al., 1998; Zanoni, 2010; Zanoni et al., 2008). The Periadriatic line nucleated due to the contrasting rheology between rocks of the Southalpine domain and rocks of the Austroalpine and Penninic domains, during Alpine nappe structural development (Figure 1(a)). West of the western segment of the Periadriatic line (Canavese line) Oligocene igneous rocks form the Biella and Traversella km-sized plutons (Bigioggero et al., 1994; Pagliani Peyronel, 1959; Van Marke de Lummen & Vander Auwera, 1990; Zanoni, 2010; Zanoni et al., 2008; Zanoni, Spalla, & Gosso, 2010) and andesitic dykes and lava flows (Callegari et al., 2004; De Capitani, Fiorentini Potenza, Marchi, & Sella, 1979;

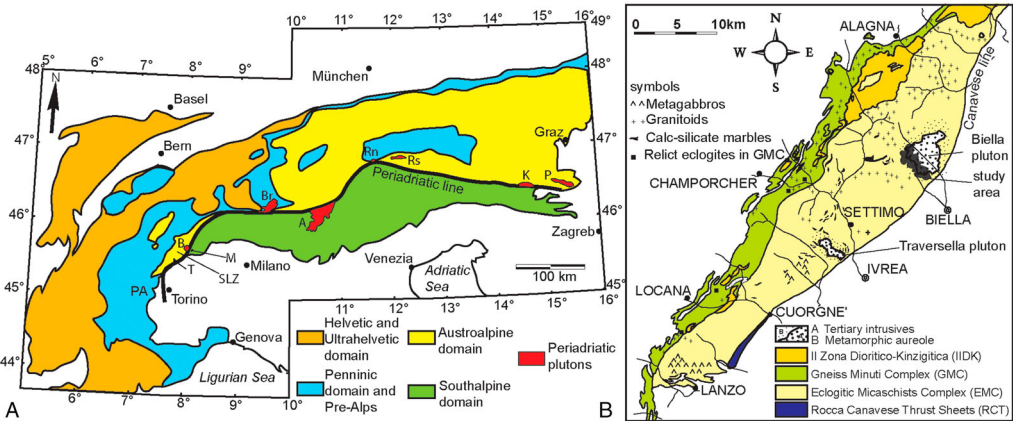


Figure 1. (a) Simplified tectonic outline of the Alps modified from Handy, Babist, Wagner, Rosenberg, and Konrad (2005) and references therein. The main Periadriatic plutons are represented as follows: T = Traversella; B = Biella; M = Miagliano; Br = Bergell; A = Adamello; Rn = Rensen; Rs = Rieserferner; K = Karawanken; P = Pohorje. SLZ = Sesia-Lanzo Zone. (b) Simplified geological map of the SLZ after Compagnoni, Dal Piaz, Hunziker, Gosso, Lombardo, and Williams (1977), Passchier, Urai, Van Loon, and Willimas (1981), and Spalla and Zulbati (2003); the mapped area is denoted by the grey shading.

Downloaded by [Politecnico di Milano Bibl] at 05:06 25 March 2016

Kapferer et al., 2012). East of the Canavese line Oligocene igneous rocks are represented by the smaller Miagliano pluton (Berger et al., 2012 and references therein). The Biella pluton, which is also known as the Valle del Cervo pluton, shows a concentric zoning in which the outer part consists of monzonite grading to syenite and the inner part consists of granite (Bigioggero et al., 1994 and references therein). The Biella and Traversella plutons are ~30 Ma (Berger et al., 2012; Bigioggero et al., 1994; Krummenacher & Evernden, 1960; Romer et al., 1996) and are emplaced in the internal Sesia-Lanzo Zone of the western Austroalpine domain (Figure 1(b)), which shows a pervasive structural imprint under eclogite facies conditions (Delleani, Spalla, Castelli, & Gosso, 2012, 2013; Giorgetti, Tropper, Essene, & Peacor, 2000; Koons, 1986; Rubbo, Borghi, & Compagnoni, 1999; Tropper & Essene, 2002; Tropper, Essene, Sharp, & Hunziker, 1999; Zucali, 2002; Zucali & Spalla, 2011; Zucali, Spalla, & Gosso, 2002) dated 60–80 Ma (Bussy, Venturini, Hunziker, & Martinotti, 1998; Cenki-Tok et al., 2011; Roda, Spalla, & Marotta, 2012; Rubatto, Gebauer, & Compagnoni, 1999; Rubatto et al., 2011) and related to the Alpine subduction. The Sesia-Lanzo Zone preserves scattered granulite to amphibolite facies relicts, which are related to Permian-Triassic lithospheric thinning that predates the Alpine convergence (Cenki-Tok et al., 2011; Lardeaux & Spalla, 1991; Rebay & Spalla, 2001; Spalla et al., 2014). After the Biella pluton emplaced, the inner part of the Sesia-Lanzo Zone was rotated southeastward about an axis parallel to the Canavese line (Lanza, 1977). Due to this rotation, deeper portions of the pluton are observed moving from the Canavese line towards the northwest. This interpretation is consistent with the variations of emplacement pressure values estimated from NNW to SSE across the pluton (Zanoni, 2007).

3. Mapping method and representation

At 1:10,000 scale, the map synthesises, the structural and petrographic data produced during the original mapping at 1:5000 scale, mostly over field seasons in 2004 and 2005. The topographic basemap is provided by the Regione Piemonte Administration. The map shows the actual outcrops and interpreted lithostratigraphy below the Quaternary cover, which is based on the location of outcrops, the rock types that form detrital deposits, and the orientation of the structural features. In both plutonic and country rocks, structural analysis enabled definition of the timing relationships between the intrusion and the deformation stages, which are represented on the map by foliation trajectories. As the Sesia-Lanzo Zone rocks are analysed where pre-intrusive mineral assemblages are variably affected by the contact metamorphism, the correlation of ductile structures is dependent on geometric criteria (e.g. Williams, 1985) but also utilises mineral assemblages that define fabrics (e.g. Hobbs, Ord, Spalla, Gosso, & Zucali, 2010; Spalla, Zucali, di Paola, & Gosso, 2005) where the effect of contact metamorphism is weak. Field mapping and structural analysis are supplemented and reinforced by the optical and electronic microscopy analyses (Blenkinsop, 2000; Passchier & Trouw, 2005; Paterson, Vernon, & Tobisch, 1989; Vernon, 2004), which enabled the variation in the contact metamorphic re-crystallisation in the different country rock types at different distances from the pluton margin to be described. The variation in the contact metamorphism effect is described in terms of contact metamorphic mineral assemblages and their modal amount and is represented on the map by increasing colour intensity of the less transformed country rocks. The microscale analysis applied to intrusive rocks allowed inferring the magmatic crystallisation order and the type of deformation that affected the igneous rocks.

4. Rock types

The following sections provide brief descriptions of igneous and country rock types. Detailed information about mineral phases and microstructures are displayed in Tables 1 and 2.

Table 1. Microstructural features of the igneous rocks.

Minerals	Rock type					
	Monzonites	Syenites with Amp	Syenites without Amp	Mafic monzonites	Aplites	Granitic veins
Kfs	SPO of euhedral phenocrysts, with Carlsbad twinning, perthites, and locally flame perthites, defines the magmatic foliation. Pl is enclosed and rims show myrmekites	Ab exsolutions, rare microcline twinning, and Pl crystals enclosed	Large euhedral phenocrysts with Carlsbad twinning and SPO parallel to the magmatic foliation	Subedral poikilitic up to mm-sized crystals enclosing Bt, Cpx, Pl, Amp, Ap (Figure 2(f)). Locally faint flame perthites	Euhedral crystals with scarce internal deformation. SPO defines a magmatic foliation that is weak in syenitic dykes	SPO of euhedral crystals defines a magmatic foliation. Crystals show undulose extinction, perthites, and flame perthites
Pl	Euhedral crystals with polysynthetic twinning and growth concentric zoning. PII: slight undulose extinction, oblique to Kfs SPO and lobate grain boundaries with Ab rim. PIII: SPO parallel to that of Kfs. PIII: myrmekites with Qz at the Kfs rim. Fine-grained Ep and Wm overgrew PII and PIII	Euhedral to subedral crystals. Crystals show irregular rim due to corrosion sealed by new growth of Ab. Crystals SPO defines a faint magmatic foliation	Polysynthetic twinning in PII and PIII. PII: crystals with rounded edges oblique to the magmatic foliation and enclosed in Kfs phenocrysts. PIII: euhedral crystals with SPO parallel to the magmatic foliation either enclosed or not in Kfs	Euhedral to subedral crystals with polysynthetic growth twinning. Local corrosion rims and frequent enclosed in Kfs. Fine-grained aggregates of Ep and Wm overgrew Pl	Enclosed in Kfs and overgrown by rare Ep	Crystal SPO parallel to the magmatic foliation
Bt	Coarse-grained crystals with kink-bands in a few cases. Locally widely replaced by Chl and minor Ep	Euhedral and minor interstitial crystals rarely with undulose extinction and kink bands and replaced by Chl	Euhedral crystals that can have interstitial edges	Euhedral crystals mostly enclosed in Kfs with SPO parallel to the magmatic foliation. Partly replaced by Chl	Widely replaced by Chl	Very rare

Amp	AmpI interstitial but locally also euhedral crystals parallel to the magmatic foliation. Often overgrew Cpx along edges or cleavages. Locally weak undulose extinction. AmpI rimmed by AmpII or Chl	Crystals parallel to the magmatic foliation		AmpI subhedral crystals with SPO parallel to the magmatic foliation or interstitial crystals between Bt laths. AmpII with minor Chl replaced AmpI	AmpI forms interstitial crystals and replaces Cpx. AmpII replaces AmpI	
Cpx	Euhedral to subhedral crystals	Very rare	Euhedral to subhedral crystals locally enclosed in Bt crystals. It is very pristine and replaced by very rare Amp	Euhedral to subhedral crystals with polysynthetic twinning and partly replaced by AmpI. Locally it encloses Bt and Ap	Euhedral to subhedral crystals diffusely replaced by AmpI	Replaced by Amp
Qz	Interstitial crystals also in sub-magmatic fractures of Kfs and PlII crystals. Often slight undulose extinction	Interstitial and coarse-grained crystals	Interstitial mono-crystals	Interstitial mono-crystals	Interstitial mono-crystals and locally shows internal deformation	Interstitial crystals between Kfs grains and sub-rounded subhedral crystals
Mag	Enclosed in AmpI	Euhedral crystals	Euhedral to subhedral crystals	Euhedral crystals	Enclosed in Kfs	
Ap	Mostly euhedral crystals enclosed in AmpI		Sub-rounded crystals	Sub-rounded crystals		
Ttn	TtnI: enclosed in AmpI. TtnII: μm -thick films between Ap and Mag	Euhedral crystals in contact with Qz, Bt, and Mag and, if enclosed in Kfs, dendritic crystals		Fine-grained crystals	Interstitial between Kfs and Pl	

Note: Mineral abbreviations after [Whitney and Evans \(2010\)](#), with the exception of white mica (Wm).

Table 2. Microstructural features of the country rocks.

Assemblages	Rock type					
	Metapelites	Meta-aplites	HT orthogneisses (a)	HT orthogneisses (b)	HT orthogneisses (c)	HP orthogneisses
Pre-intrusive assemblages	HP: WmI and II, Qz, OmpI and II, Rt, GrtI, AmpI (Gln or Hbl), Ep, Ttn. LT: ChII, Ab, WmIII, rare AmpII (Act)	HP: Qz, WmI and II, Kfs, rare Gln and Grt. LT: ChII and Ab	HT: Qz, BtI, PlI, KfsI (porphyroclast), KfsII, WmI (porphyroclast; Figure 5(b))	Anatectic: Qz, KfsI, Wm, \pm Grt. HT: Qz, KfsII, PlI	HT: Qz, BtI, PlI; HP: Qz, WmI, Rt, Omp	HP: Qz, Wm, Grt, Kfs, Omp, EpI, Rt
Contact metamorphic assemblages and degrees of transformation	Poorly affected	Rare Bt grew along [001] surfaces or rim of WmI and II and in GrtI fractures and at the expenses of WmIII and ChII. Ilm rims Rt. Omp completely replaced by a fine-grained aggregate of Bt and Pl (Figure 4(a))	Fine-grained Bt along [001] surfaces of WmI and II			
	Partly affected	WmI and II partly replaced by Bt, Pl, and Crd (Figure 4(b)). Bt rims AmpII and, with Pl, Grt. Pl and Kfs form aggregate parallel to the rock fabric. Qz forms polygonal aggregates. EpI rimmed by (REE-rich) EpII	Wm partly replaced by Bt. Layers of polygonal coarse-grained Qz and finer-grained granoblastic Pl mimic the rocks fabrics	Qz forms layers of partially recrystallised grains	BtI recrystallised and fine-grained BtII partly replaced WmI (Figure 5(e)). Omp is completely replaced by a very fine-grained aggregates possibly consisting of BtII and PlII. Rt is rimmed by Ilm	Qz shows a nearly complete polygonal structure. Wm is rimmed by Bt and EpI by EpII. Fine-grained Bt and Pl rim Grt. Omp is replaced by WmII, EpII, and minor Pl (Figure 5(f)). Rt is rimmed by Ilm

Affected	Up to 400 m from the pluton Wm is partly replaced by Crn, Bt, and Crd or by Bt, Pl, and And. Up to 250 m from the pluton Crn, Crd, and Pl aggregate occur and Bt rims AmpI. EpII more pervasively replaced EpI. Wm is partly preserved, but in the Desate area Wm is fully replaced at larger distances. Qz, Pl, and Bt form granoblastic aggregates mimicking the rock fabric. In Qz aggregates polygonal structures are well developed and single grains are free of internal deformation. Up to 100 m from the pluton Wm is also replaced by Spl. And forms mm-sized crystals in grabolastic aggregates of Crd rimmed by Pl. Here Bt forms rosettas rounded aggregates of coarser-grained crystals that include Ilm. Up to a few dozens of metres from the pluton Omp is replaced by Opx, Bt, Pl and Qz and aggregates of GrtII, Crd, Bt. By the contact Sil, Kfs, Bt and Crd formed	Strain-free Qz crystals form polygonal layers mimicking rocks fabrics. Wm I and II are completely or pervasively replaced by Pl, And, Bt, Crd, and Crn, whereas by the pluton there is Spl instead of Crn. Bt mostly is concentrated along margin whereas Pl and Crd are abundant in the core of ex-Wm. ChII is partly replaced by Bt (Figure 4(d)). Grt is rimmed by coronitic Bt and Pl. At a few metres from the pluton WmI and II is replaced also by Sil and Kfs	Qz shows recrystallised sub-grains free of internal deformation. WmI is replaced by Bt and Crn. KfsII and PII layers recrystallised into KfsIII and PIII with increasing of the grain size. BtII contains globular Ilm. Very close to the margin layers containing BtII, Crd, KfsIII, PIII, Ilm, and Sil occur (Figure 5(c))	BtII weakly replaced Wm and Grt. Both phases are still well preserved. Wm is replaced also by rare Crn	Fine-grained BtI, Ilm, and Pl form layers mimicking the pervasive foliation. Wm is rarely preserved and is replaced by Bt and Pl. Qz forms polygonal structures of strain-free grains. Rt is replaced by Ilm
Partial melting	Up some dozens of metres from the pluton. Coarse-grained sub-rounded Qz crystals with interstitial Kfs and Pl. Interstitial Qz between euhedral Kfs and Pl. Coarse-grained WmIV enclosing Kfs and Bt or interstitial WmIV between Qz crystals. Euhedral Crd in contact with Qz (Figure 4(c)) or Kfs				
Post-intrusive assemblages	ChIII \pm saagenitic Rt overgrew Bt. ChII and WmIV (pinite) replaced Crd. EpIII and WmIV (saussurite) replaced Pl	Fine-grained WmIII overgrew Pl and ChIII and WmIII \pm Ttn \pm saagenitic Rt overgrew Bt	Fine-grained WmII overgrew Crn	Ab grew between KfsII and PII	

Note: Mineral abbreviations after Whitney and Evans (2010), with the exception of white mica (Wm).

4.1. Igneous rock types

Igneous rocks of the southwestern Biella pluton consist of monzonites and quartz-monzonites with minor syenites and quartz-syenites and even rarer mafic monzonites. Aplitic dykes and granitic veins intersect these rocks.

4.1.1. Monzonites

The monzonites consist of: K-feldspar (41–25%), plagioclase (33–26%), biotite (17–5%), amphibole (17–4%), clinopyroxene (14–7%), quartz (13–7%), magnetite (0.5–1.5%), titanite (0.3–1%), and apatite (0.2–0.3%). These coarse- to medium-grained rocks contain a magmatic foliation that is indicated by SPO (shape preferred orientation) of K-feldspar and plagioclase (Figure 2(a)). They frequently enclose country rock xenoliths (Figure 2(b)) and rare magmatic mafic enclaves (Figure 2(c)). Xenoliths preserve the ghost country rock foliation whose defining minerals are replaced by biotite and quartz-feldspar. Locally at the contact with the country rock, monzonites are fine-grained and richer in biotite. The contact with the country rocks may be gradual, where monzonites intrude along the foliation surfaces of country rocks (Figure 2(d)), and sharp, where monzonites cut country rock foliation (Figure 2(e)). Details about microstructures are presented in Table 1. Dm-sized xenoliths are prevalent in the southern part of the map. These xenoliths are elongated parallel to the foliation they contain, which is a weak surface along which country rocks preferentially break and transform into tabular shaped blocks. The tabular shape of xenoliths facilitates their orientation parallel to the magmatic foliation (Figure 2(b)). In place, these features suggest scarce assimilation of country rock material by the monzonitic magma (according to Fiorentini Potenza, 1969) and that the country rock structure has a strong influence on xenolith formation and shape.

4.1.2. Syenites

Two types of syenites were recognised. (1) Syenites with amphibole are medium- to coarse-grained locally pegmatitic rocks, including K-feldspar ~56%, plagioclase ~21%, quartz ~12%, biotite ~5%, amphibole ~3%, clinopyroxene ~1%, magnetite ~1%, titanite ~1%. (2) Syenites without amphibole are medium-grained rocks, including K-feldspar ~41%, plagioclase ~18%, clinopyroxene ~15%, biotite ~14%, quartz ~10%, magnetite ~1%, apatite ~1%. Usually the contact between syenites with amphibole and monzonite is gradual and only locally is clear.¹ The contact between syenites without amphibole and monzonites is usually sharper than the previous one and is evident along the road just north of Testette (Main Map).

4.1.3. Mafic monzonites

These rocks consist of K-feldspar ~22%, plagioclase ~22%, biotite ~21%, amphibole ~20%, clinopyroxene ~9%, quartz ~2.5%, apatite ~2%, titanite ~1%, and opaque minerals ~0.5%. At the contact with monzonite biotite (~36%), clinopyroxene (~18%), quartz (~8%), apatite (~2.5%), and opaque minerals (~1.25%) increase, whereas K-feldspar (~17%), amphibole (~11%), plagioclase (~6%), and titanite (~0.25%) decrease. Locally these rocks contain patches of abundant amphibole (~65%) and minor K-feldspar (~21%), plagioclase (~7%), apatite (~3%), titanite (~2%), and quartz (~2%). They form dm- to m-sized rounded bodies in the monzonites and contain a magmatic foliation that is defined by SPO of biotite and clinopyroxene (Figure 2(f)). A large body surfaces at Cima Tressone (Main Map). The soft contact of smaller mafic enclaves against monzonites suggests a low rheological contrast between the

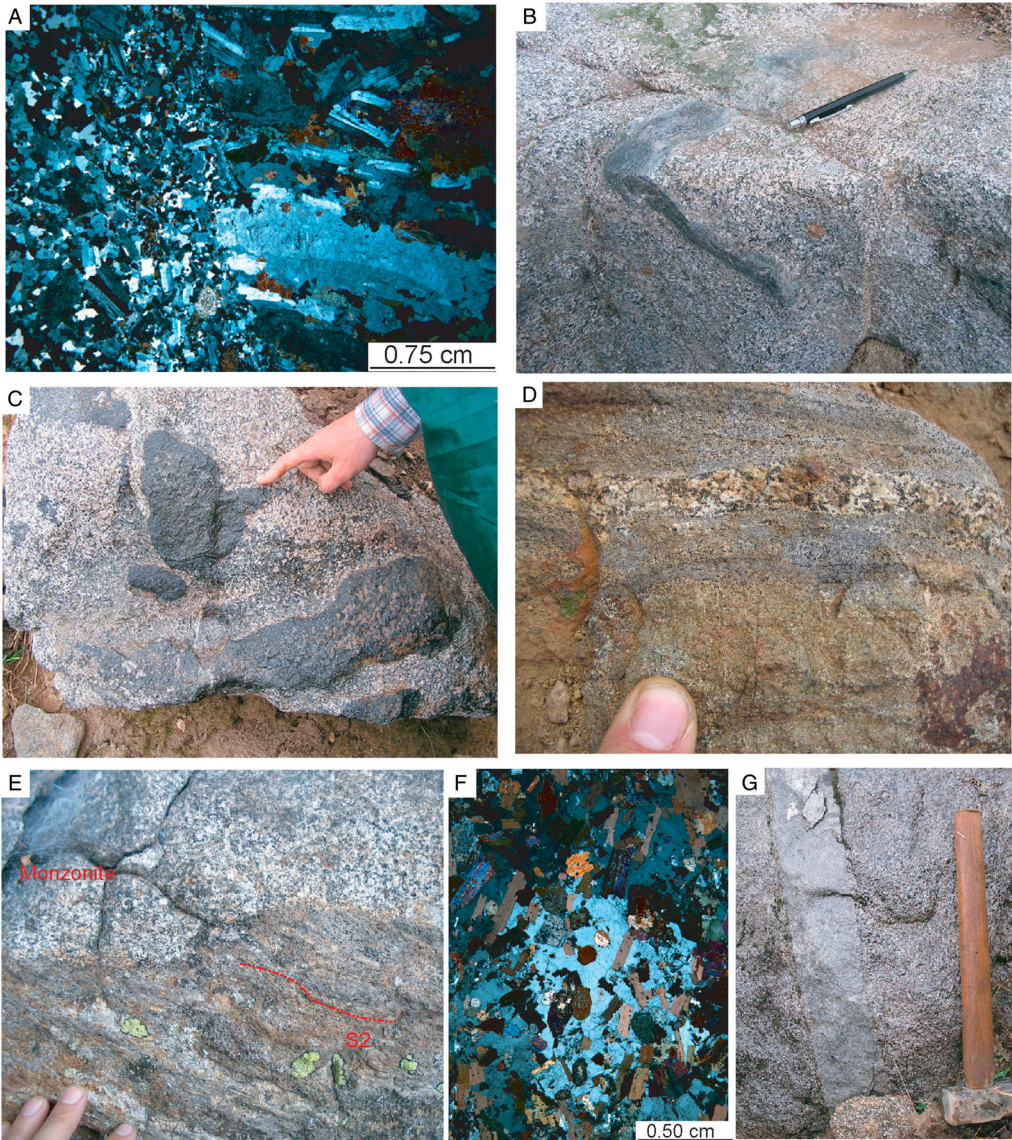


Figure 2. (a) K-feldspar and plagioclase II, which display SPO that defines the magmatic foliation in monzonite. This foliation is intersected by an aplitic dyke with a magmatic foliation parallel to and better developed at the contact with monzonite. Crossed polars. Sample from the northeastern ridge of M. Becco at 1630 m asl. (b) Tabular xenolith of country rocks parallel to the magmatic foliation of monzonite. East south-east of C.^{na} Cortetto at 1220 m asl. (c) Soft contacts of mafic enclaves and monzonite. Monzonite near the enclaves is enriched in mafic minerals possibly by mixing. Northeastern slope of Cima Tressone at ca. 1580 m asl. (d) Monzonite intruded along regional S2 foliation in transformed metapelites. Northeast of Pian del Lotto at 1340 m asl. (e) Regional S2 foliation in transformed metapelites intersected by intrusive contact of monzonite. South southeast of Tempietto at ca. 1370 m asl. (f) Poikilitic K-feldspar enclosing euhedral biotite and clinopyroxene, which define the magmatic foliation in mafic monzonite; crossed polars. Cima Tressone ridge. (g) Sharp aplitic dyke in monzonite. Northeastern slope of Cima Tressone at ca. 1600 m asl.

two rocks and indicates that the two rocks were a crystal mush when mechanically interacted. Their subspherical shape is consistent with a small amount of magmatic deformation (e.g. [Tobisch & Williams, 1997](#)). Near these enclaves, monzonite is enriched in mafic minerals along shaded bands that are parallel to the magmatic foliation ([Figure 2\(c\)](#)). These shaded bands may be due to magma mingling and magmatic flow. Hornblenditic enclaves are wrapped by the magmatic foliation of monzonite; therefore, they were already solid or contained less than 7% of melt (e.g. [Rosenberg & Handy, 2005](#)) when embodied in monzonitic magma.

4.1.4. *Aplitic dykes*

Cm- to dm-thick dykes sharply intersect the monzonites ([Figure 2\(g\)](#)) and outcrop to m-long exposures. These fine-grained rocks have a syenitic to granitic composition and consist of K-feldspar (59–41%), plagioclase (16–14%), quartz (12–33%), amphibole (7–5%), biotite (6–2%), clinopyroxene (1–0%), titanite (2–0%), and opaque minerals (2–0%). The dykes intersect ([Figure 2\(a\)](#)) or are parallel to the magmatic foliation of hosting monzonites and contain a magmatic foliation that is parallel to the dyke wall. These features are consistent with dyke emplacement after monzonite cooling.

4.1.5. *Granitic veins*

Monzonites are crosscut by granitic veins with a thickness of a few cm. These veins primarily consist of K-feldspar (~46%), quartz (~40%), plagioclase (~13%), biotite, and clinopyroxene (~1%). These veins contain a magmatic foliation at a high angle with the vein wall. Magmatic foliation of the veins is parallel and continuous to the magmatic foliation in hosting monzonites. These features may suggest that these veins opened and gathered residual melts during cooling of monzonite.

As indicated by the microstructural features synthesised in [Table 1](#), the igneous rocks of the southwestern Biella pluton contain a pervasive magmatic foliation defined by euhedral crystals without or with scarce internal deformation. The crystallisation order of magmatic phases is generally characterised by an initial growth of plagioclaseI and clinopyroxene followed by a growth of K-feldspar, plagioclaseII, biotite, amphiboleI and late quartz crystallisation (see [Figure 3](#) for more details).

4.2. *Country rock types*

The country rocks of the southwestern Biella pluton consist of metapelites with minor meta-aplites and HT (high temperature) and HP (high pressure) metagranitoids. With the exception of HT metagranitoids, all country rock types show pre-intrusive pervasive assemblages, which are characteristic of eclogitic facies conditions. Country rocks are variably affected by the contact metamorphism. On the map, at distances between 350 and 900 m from the contact with plutonic rocks, the country rocks contain less than 30% of contact metamorphic minerals, which are only visible at the microscale. Between 100 and 800 m from the pluton boundary, the country rocks contain a maximum of 70% of contact metamorphic minerals and preserve pre-intrusive assemblages. At maximum distances of 400 m from the pluton, the country rocks are significantly transformed by the contact metamorphism and contain more than 70% of contact metamorphic minerals. However, relicts of pre-intrusive minerals may still be visible at the microscale. Even where rocks are significantly affected by contact metamorphism, the ghost traces of the pre-intrusive foliations are visible at the mesoscale.

	Monzonite		Syenite with Amp		Amp-free Syenite	Mafic Monzonite	
	magmatic	post-magmatic	magmatic	post-magmatic	magmatic	magmatic	post-magmatic
Cpx	—		—		—		
Pl	I — II —	III —	—		I — II —		
Kfs	—		—		—	—	
Amp	I —	II —	I —		—	I —	II —
Bt	—		—		—	—	
Mag	—		—		—	—	
Ttn	I — II —		—				
Ap	—				—		
Qz	—		—		—	—	
Chl							—
Ep							—
Wm							—

Figure 3. Possible magmatic crystallisation order and successive sub-solidus recrystallisation in the igneous rock types of the Biella pluton, as deduced by microstructural analysis. Mineral abbreviations after [Whitney and Evans \(2010\)](#), with the exception of white mica (Wm).

4.2.1. *Metapelites*

Metapelites are the most diffused country rock type and consist of micascists and paragneisses with meta-aplite layers. Meta-aplite layers have variable thickness and are only mappable in the Cima Cucco area. Metapelites also contain metabasic boudins that are dm-sized in the Cima Cucco area and to the east of Oropa and are m-sized to the west of C. Orsuccio. The main minerals that form metapelites include white mica, quartz, feldspar, garnet, omphacite and amphibole. On the map, up to ca. 800 m from the pluton margin, metapelites are affected by the contact metamorphism, shown by the increase in fine-grained biotite closer to the pluton. Near the pluton metapelites are completely transformed by contact metamorphism and locally (along the ridge between Cima Tressone and Monte Tovo or near A. Pera) metapelites are enriched in quartz possibly due to the circulation of fluids generated by igneous rock crystallisation or contact metamorphic reactions (for details refer to [Table 2](#) and [Figure 4\(a–c\)](#)).

4.2.2. *Meta-aplites*

Meta-aplites consist of quartz, feldspar, white mica, and glaucophane. Up to cm-sized white mica crystals and quartz-feldspar layers define the pervasive foliation. Ghost mm-sized white mica crystals protrude from the outcrop surface having become harder than the rock matrix from the contact metamorphic transformations. At the same distance from the pluton, metapelites are more transformed than meta-aplites, as better-preservation of white mica and garnet in the last rocks suggests (see [Table 2](#) and [Figure 4\(d\)](#) for details).

4.2.3. *HT metagranitoids*

Along the Pragnetta valley, upstream with respect to S. Giovanni, and north of Desate (see the Main Map), metagranitoids that preserve HT fabrics occur. These rocks contain a pervasive foliation that is defined by quartz-feldspar layers and biotite-rich layers and transposed meta-aplites. West of S. Giovanni, these metagranitoids are associated with kinzigites and metabasic lenses and display a mylonitic foliation. The mylonitic foliation is intersected by meta-aplitic dykes with walls that are pinched in the foliation surfaces ([Figure 5\(a\)](#)), which suggests that they intruded during incremental mylonitisation. More details on microstructures are included in [Table 2](#) and [Figure 5\(b\)](#) and [5\(c\)](#). Meta-aplites consist of quartz, feldspar, and white mica. North of Desate these rocks occur in mappable sizes and intersect the pervasive foliation. North of C. Boriom

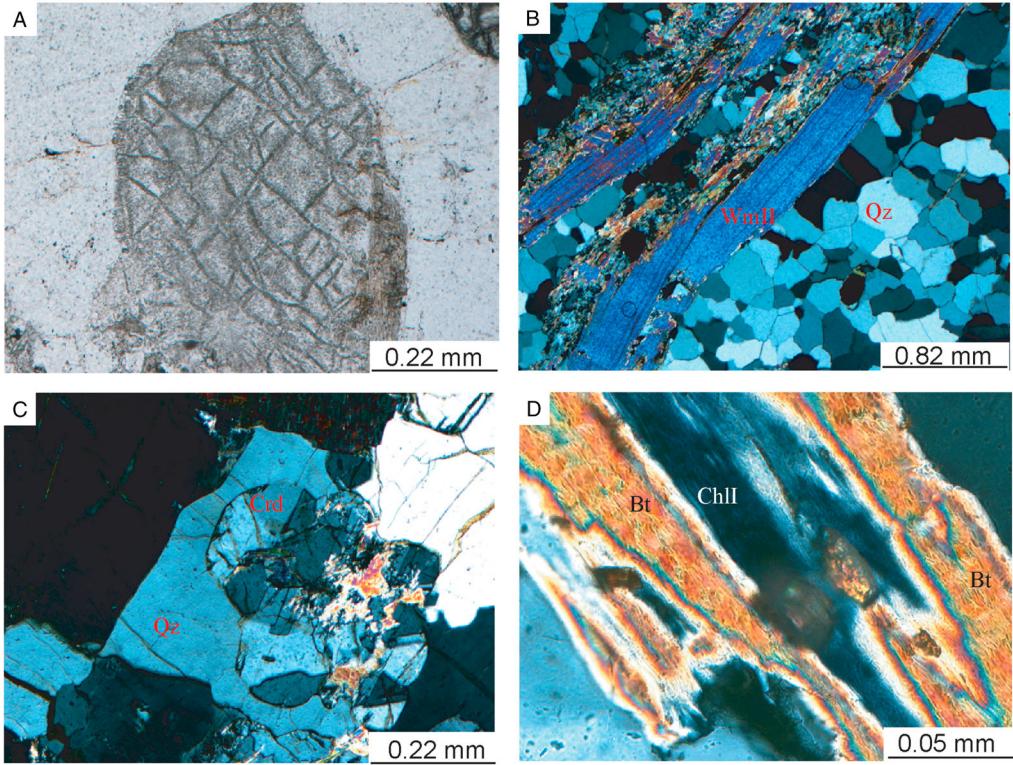


Figure 4. Metapelites and meta-aplites affected by contact metamorphism. (a) Omphacite replaced by very fine-grained biotite and plagioclase in metapelite. Plane polarised light. Sample from the trail south south-west of Tempietto at ca. 1180 m asl. (b) White micaII partly replaced by cordierite, biotite and plagioclase in partly transformed metapelite. Quartz shows incipient polygonal structure. Crossed polars. Sample from the eastern ridge of Monte Tovo at ca. 1980 m asl. (c) Euhedral cordierite crystals in contact with interstitial quartz, in transformed metapelite. Crossed polars. Sample from the north of C. Orsuccio at ca. 1700 m asl. (d) ChloriteI rimmed by contact metamorphic biotite in transformed meta-aplite. Crossed polars. Sample from the north northeast of Pian del Lotto at ca. 1450 m asl. Mineral abbreviations after [Whitney and Evans \(2010\)](#), with the exception of white mica (Wm).

and S. Giovanni, rocks with migmatitic structures are associated with HT metagranitoids. HP minerals, such as white mica and possibly omphacite, overprint these structures ([Figure 5\(d\)](#)) and in turn are overprinted by contact metamorphic minerals ([Figure 5\(e\)](#)). Locally, these rocks grade into metapelites north of S. Giovanni. In HT metagranitoids, the contact metamorphism is usually weaker compared with other rocks at the same distance from the pluton (see [Table 2](#) for details).

4.2.4. *HP metagranitoids*

These rocks only outcrop in the northwestern corner of the map and are characterised by coarse-grained white mica and omphacite, which defines the pervasive foliation. These rocks appear similar to the green metagranitoids in the southern slope of Monte Mucrone as described by [Delleani et al. \(2013\)](#). The contact metamorphism in the HP metagranitoids is responsible for the replacement of white mica by biotite and the nearly complete replacement of omphacite even at outcrops where white mica is quite fresh (see [Table 2](#) and [Figure 5\(f\)](#) for details).

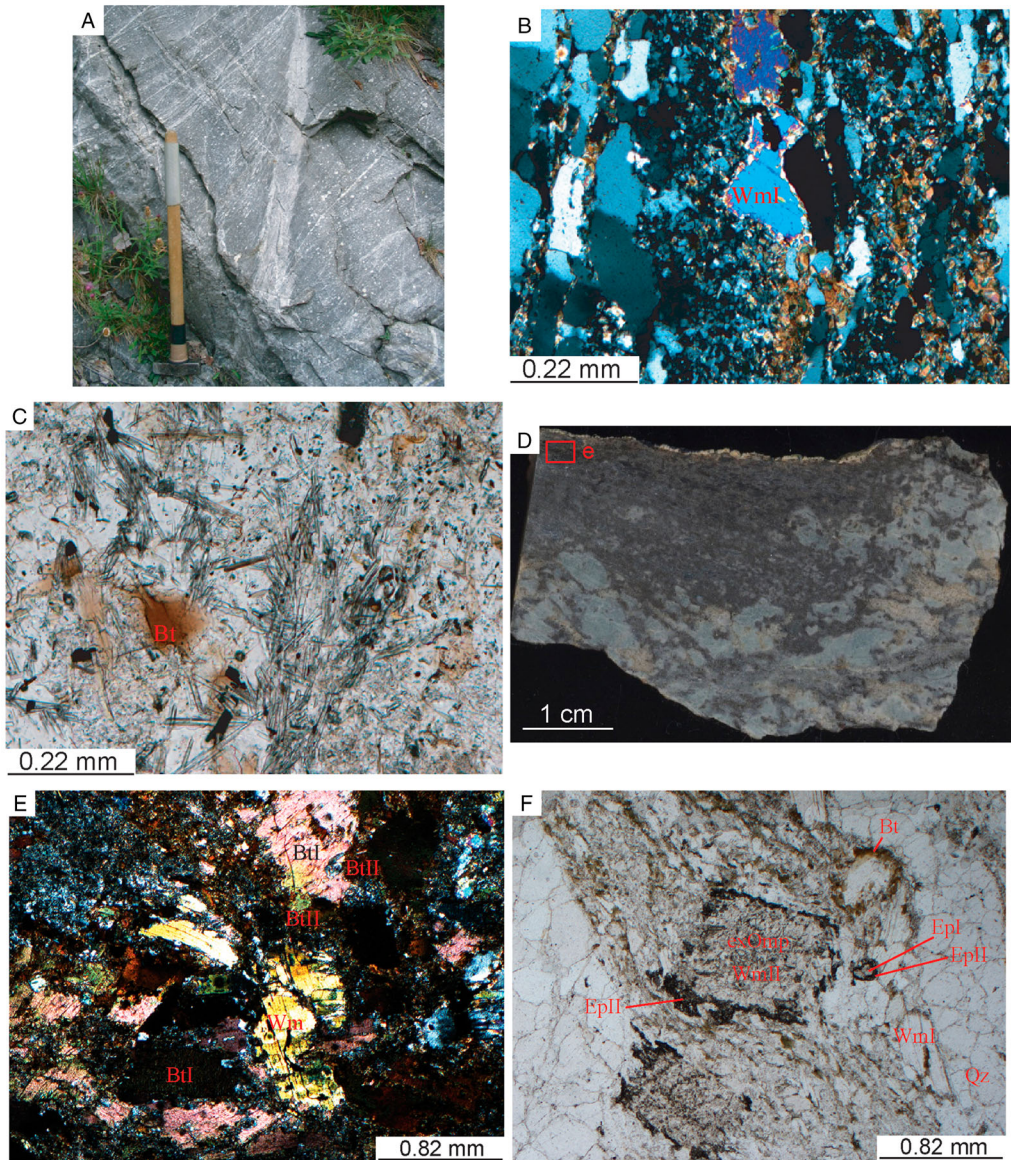


Figure 5. Metagranitoids. (a) Meta-aplitic dyke interdigitated with mylonitic foliation in HT metagranitoid. Pragnetta torrent west of S. Giovanni at ca. 1200 m asl. (b) White mical porphyroclast wrapped by the S1p mylonitic foliation in HT metagranitoids in partly transformed HT metagranitoids; crossed polars. Sample from the Pragnetta torrent west of S. Giovanni at 1220 m asl. (c) Fine-grained aggregate of biotiteII, sillimanite, cordierite, K-feldspar, quartz in transformed HT metagranitoids; plane polarised light. Sample from the north of Desate at 1200 m asl. (d) Scan of a rock slab that shows a diatexite-like structures. Biotite-rich layer (black) represents the restitic material of diatexite. Pale blue zones consist of a fine-grained contact metamorphic aggregate replacing possibly omphacite after plagioclase. Red rectangles locate (e). (e) Biotite-rich layer defined by coarse-grained biotiteI, overprinted by coarse-grained white mica; fine-grained biotiteII overprints biotiteI and white mica; crossed polars. (f) Omphacite nearly completely replaced by white micaII, epidoteII and minor plagioclase; epidoteI is rimmed by epidoteII and white micaI by biotite; plane polarised light. Sample from the slope west of C. Boriom at 1450 m asl. Mineral abbreviations after [Whitney and Evans \(2010\)](#), with the exception of white mica (Wm).

5. Structural data

The mapped area is affected by a polyphase ductile and brittle deformation history. Throughout the mapped area, the dominant fabric is the regional S2 foliation developed in eclogite facies conditions. However, among the groups of structures that predate S2 foliation, some are characteristic of HT conditions. Ductile structures predate the intrusion of the igneous rocks, with the exception of folds and shear zones in the country rocks of the deeper part of the pluton (D7 in Table 3). Magmatic fabrics are well preserved. Brittle structures affect both plutonic and country rocks. The different groups of ductile and brittle structures are defined and numbered from older to younger based on overprinting relationships. The groups of ductile structures associated with HT metamorphic conditions are interpreted as pre-Alpine (e.g. Lardeaux & Spalla, 1991); their numbering is accompanied by a lowercase 'p', which denotes pre-Alpine. Acronyms for the ductile structures are provided in the caption for Table 3.

5.1. Ductile structures

Ductile structures are only recorded in the country rocks and are classified into nine groups (Table 3).

5.1.1. Pre-Alpine deformation

A pre-Alpine evolution is recognised just in the HT-metagranitoids and is characterised by two groups of structures. *D1p* consists of rare *D1p* tight folds to isoclinal folds (Figure 6(a)) and the *S1p* axial plane foliation. *S1p* is the pervasive structure in the HT-metagranitoids and mostly is a mylonitic or gneissic foliation. *D2p* consists of the *SZ2p* shear zone, which intersects the *S1p* foliation (Table 3).

5.1.2. Alpine deformation

The Alpine deformation is dominant in all rock types with the exception of HT-metagranitoids. Among the Alpine deformation stages, only *D1*, *D2*, and *D5* produced a schistosity. *D1* consists of an *S1* foliation, which is recorded in metapelites and meta-aplites, and *D1* folding, which is recorded in HT metagranitoids and locally in metapelites. *D1* folds are open in HT metagranitoids (Figure 6(a)) and are isoclinal in metapelites and meta-aplites (Cima Cucco and NW of P.^{ta} Maro). *D2* consists of *S2* foliation and *D2* folding, which are recorded in metapelites, meta-aplites, and HP metagranitoids. *D2* folding usually comprises tight to isoclinal folds (Figure 6(b)). *D2* folding is rarely recorded in HT metagranitoids. *D3* consists of *D3* folding, which is recorded in metapelites nearby Oropa and A. Pera and forms tight folds. *D4* consists of cm-thick *SZ4* shear zones that are recorded in metapelites near A. Pera (Figure 6(c)) and the road between Oropa and Tempietto. *D5* consists of *D5* open folds in metapelites (Figure 6(d)) and meta-aplites and a local *S5* crenulation foliation (Figure 6(e)) in metapelites near Oropa. *D6* consists of upright open *D6* folds in metapelites, meta-aplites, and locally HT metagranitoids (Figure 6(f)). *D7* consists of tight *D7* folds in metapelites and *SZ7* shear zones in HP metagranitoids near Desate.

5.2. Magmatic structures

Igneous rocks of the southwestern Biella pluton display a magmatic foliation (*Sm*) and lineation (*Lm*) that are defined by SPO of K-feldspar and plagioclase and minor amphibole and biotite. In the southern part of the map, *Sm* is also defined by preferred orientation of xenoliths. *Sm* is steep, dips NW-, NE-,

Table 3. Features of ductile meso-structures.

Group of structures	Fabric element	Description	Main orientation	Metamorphic facies
D1p	S1p, AP1p, A1p; EL1p	Mylonitic foliation S1p defined by transposed meta-aplitic dykes SPO of KfsI and rare WmI porphyroclasts, PlI, Btl; Kfs shows core (KfsI) mantle (subgrains of KfsII). Meta-aplitic dykes intersect S1p and are deformed along S1p surfaces (Figure 5(a)). North of Desate Sp1 is cut by mappable meta-aplitic venis. Locally a pre-S1p foliation is preserved (Figure 6(a))	S1p: dd = NW/WSW; d = shallow to high. AP1p: dd = WSW/WNW; d = small to high. A1p: dd = SE; d = 30°; EL1p: dd = NW; d = 10 – 40°	G*
D2p	SZ2p	Ductile shear zone intersecting syn-S1p meta-aplitic dykes with a cm- to dm-sized offset. They are defined by S-C structures and kink bands. These shear zones are intersected by subsequent meta-aplitic dykes	SZ2p: dd = NE/SW, minor NE; d = small to moderate	G*
D1	S1, AP1, A1	Cm- to dm-sized isoclinal D1 folds are preserved in metapelites, and up to m-sized open to tight D1 folds are recorded in HT orthogneisses. S1 is defined by Qz, WmI, Rt, ± GrtI, ± OmpI. It is preserved in cm- to dm-sized domains and locally up to m-sized (close to Oropa) domains; in these cases S1 is defined also by transposed meta-aplites	S1: dd = SE/NW; d = variable; AP1 = dd = SW/SE; d = shallow to high; A1: dd = NW/SE; d = 20–80°	E*
D2	S2, AP2, A2	Cm- to m-sized tight to isoclinal D2 folds are coeval with the development of S2 foliation that is responsible for the almost complete transposition of previous fabrics in metapelites, meta-aplites, and HP orthogneisses. Open D2 folds are recorded in HT orthogneisses. S2 is defined by Qz, WmII, Rt, Grt, ± OmpII, ± Gln, ± Kfs, and transposed meta-aplites	S2: dd = SW/NE; d = shallow; AP2: dd = SW/NE; d = shallow (sub-vertical in HT orthogneisses); A2: dd = WSW/E; d = shallow to sub-vertical (sub-horizontal in HT orthogneisses)	E*

(Continued)

Table 3. Continued.

Group of structures	Fabric element	Description	Main orientation	Metamorphic facies
D3	AP3, A3	Dm- to m-sized and tight to open folds with rounded hinge zones	AP3: dd = NW/SE; d = 30–50°; A3: dd = E/W; d = moderate to shallow	E**
D4	SZ4	Cm-sized dextral shear zones continuous for a few metres	SZ4: dd = WSW/E; d = shallow to moderate	BS**
D5	S5, AP5, A5	M-sized open folds that develop a local S5 axial plane foliation. S5 is spaced and defined by WmIII, Chl, ± Ab	S5: dd = N; d = shallow; AP5: dd = N/S/E; d = shallow; A5: dd = NE/SW/SE; d = shallow	GS*
D6	AP6, A6	M-sized open folds with rounded hinge zone	AP6: dd = NE/SSE; d = sub-vertical; A6: dd = SE; d = sub-horizontal	GS**
D7	AP7, A7, SZ7	M-sized tight folds recorded up to 100 m far from the pluton margin with AP subparallel to the margin of the pluton and to the magmatic foliation. Shear zones marked by Qz, Pl, and Kfs ribbons wrapping Wm and possible Omp porphyroclasts	AP7: dd = WNW/NNW; d = shallow to moderate; A7: dd = E; d = 50°; SZ7: dd = WSW; d = 10–15°	Contact metamorphism*

Notes: S, foliation; AP, fold axial plane; A, fold axis; SZ, shear zone; EL, extensional lineation; dd, dip direction; d, dip. Metamorphic facies conditions.

*Assumed based on the mineral assemblages.

**Assumed by comparison with the description by [Delleani et al. \(2013\)](#), [Zucali \(2002\)](#), [Zucali et al. \(2002\)](#): G, granulite; E, eclogite; BS, blueschist; GS, greenschist. See the Main Map for lower hemisphere equal area projections of orientation data.

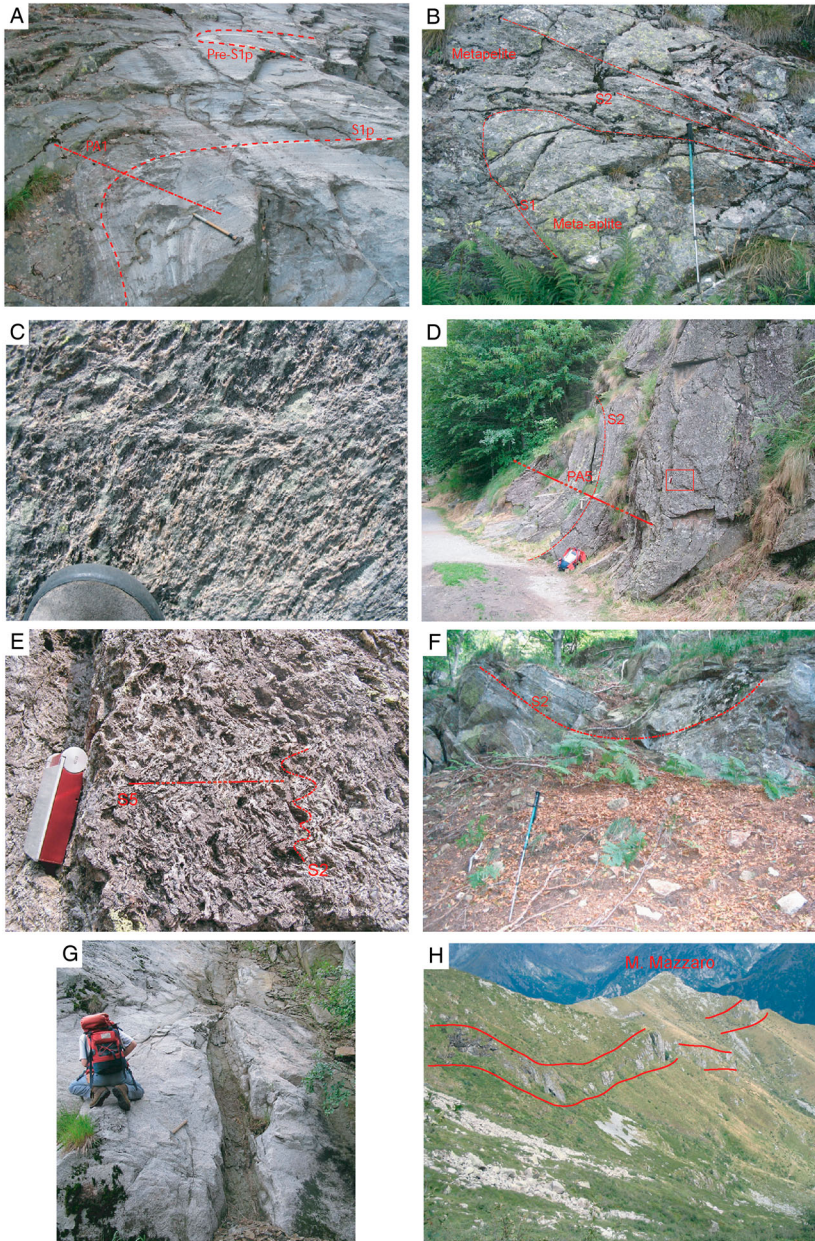


Figure 6. (a) S1p foliation in HT metagranitoid with a relict fold that is defined by pre-S1p foliation. Pragnetta torrent west of S. Giovanni at 1210 m asl. (b) D2 fold affects the contact between meta-aplites and metapelites transposed into S1. Rio S. Martino stream at 1400 m asl. (c) Dextral SZ4 in transformed metapelites at A. Pera. (d) D5 folding affects S2 in metapelites near Oropa, on the trail south southeast of Tempietto at 1200 m asl. (e) Close-up of the previous picture showing the S5 creunulation foliation. (f) D6 folding affects S2 in partly transformed metapelites near Oropa, southwest of Tempietto at ca. 1260 m asl. (g) Cataclastic band in monzonite. On the trail between Ristor. Rosazza and C.^{na} Cortetto at 1490 asl. (h) Thick cataclastic band in monzonite that propagates into the country rocks as well. Picture taken from the north-eastern slope of Monte Tovo at 1780 m asl.

and SW-ward, and is approximately concordant with the orientation of the margin with the country rocks (refer to orientation data on the Main Map). Lm mainly exhibits shallow dips and a disperse orientation. The different orientations of the pervasive S2 and Sm foliations in the country rocks and plutonic rocks, respectively, suggests that the ductile deformations in the country rocks predate the intrusion (for further details, refer to Zanoni et al., 2010; Zanoni, Spalla, Gosso, & Zucali, 2007).

5.3. Brittle structures

5.3.1. Cataclastic bands

Up to m-thick N–S trending sub-vertical cataclastic bands affect country rocks west of S. Giovanni. Thinner cataclastic bands affect metapelites west of Pian del Lotto and igneous rocks in the Cima Cucco and A. Pera areas. NW–SE and E–W trending dm-thick cataclastic bands occur in igneous rocks by Rio Rovinaie, M. Becco (Figure 6(g)), and Capanne Bele. Between Monte Tovo and M. Mazzaro, a ~10 m-thick NW-dipping cataclastic band intersects plutonic and country rocks (Figure 6(h)) and is characterised by a shallow to 50° dipping cataclastic foliation. A few S–C structures indicate that this cataclastic band accommodated a reverse sinistral movement with the possibility of transport top-to-the-south (Zanoni, 2007).

5.3.2. Fractures

Similar sets of fractures affect the country and plutonic rocks; the most frequent fractures are sub-vertical and N–S striking (see orientation data on the Main Map). The polar density plots on the map also reveal the orientation of three subsequent groups of fractures (F1, F2, and F3), which are interpreted based on the overprinting relation at single outcrops. The most dominant fracture system is F2 (Table 4). The comparison of the fracture orientations in the pluton and country rocks indicates that the magmatic cooling fractures are interpreted as sub-horizontal in the southern part of the mapped area, shallow W-dipping in the central part of the mapped area, and sub-horizontal and shallow NW-dipping in the northern part of the mapped area (Figure 7). Some fractures are filled with chlorite, chlorite and epidote, tourmaline, amphibole, and quartz. In country rocks, the mineralised fracture systems are shallow dipping or sub-horizontal, whereas quartz-bearing fractures detected within 100 m from the pluton are steep to sub-vertical. Amphibole-bearing fractures occur within 20 m, whereas tourmaline-bearing fractures within 200 m from the pluton. In plutonic rocks, chlorite-, chlorite-epidote-, and epidote-bearing fractures occur with minor tourmaline-, amphibole-, and tourmaline-epidote-bearing fractures (see the Main Map).

Table 4. Orientations of sets of pervasive fractures in the southern, central, and northern part of the mapped area in the plutonic and country rocks.

Group of fractures	Orientation	Distribution
F1	Conjugate SSW- and SSE-dipping with variable angles	Similar in plutonic and country rocks
F2	Conjugate NNE- and SSW-dipping with angles between ca. 65° and 45°, respectively. N–S trending sub-vertical	N–S trending and SSW-dipping similar in plutonic and country rocks; NNE-dipping more frequent in country rocks
F3	Conjugate NNW-dipping and E-dipping with angles of ca. 70° and 45°, respectively	NNW-dipping more frequent in pluton and E-dipping have similar frequency in plutonic and country rocks

Note: Refer to the map plate for lower hemisphere equal area projections of the orientation data.

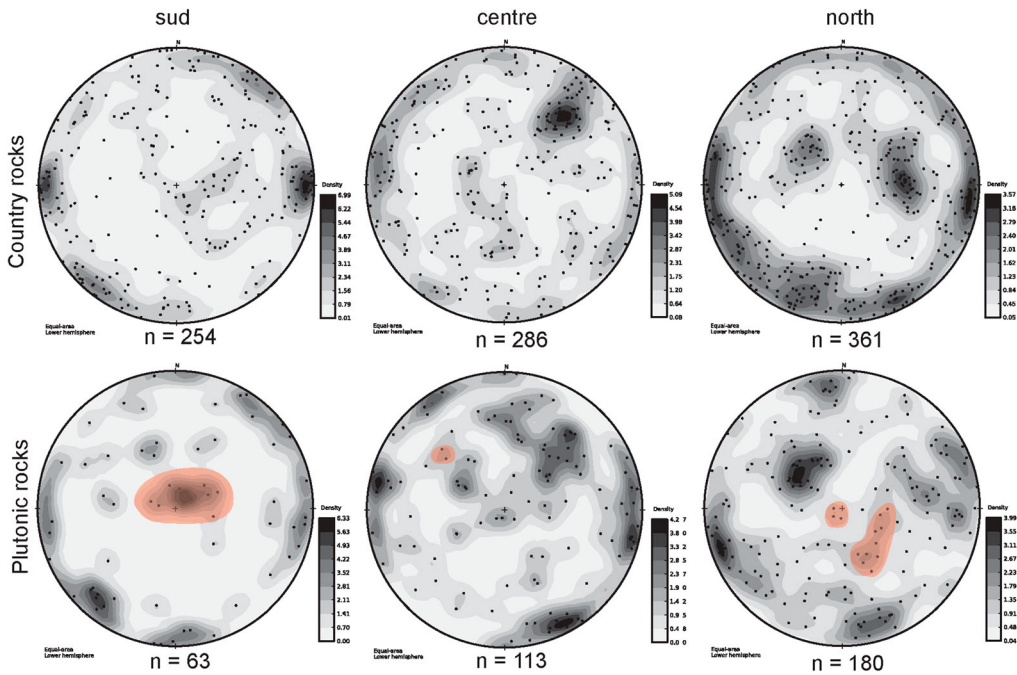


Figure 7. Orientation of fractures in the southern (M. Becco – Cima Cucco) central (area Cima Tressone – A. Pera), and northern (area between Desate and M. Mazzaro) part of the mapped area. Magma cooling fractures are interpreted based on preferential concentration in plutonic rocks and are highlighted by the red shading. ‘*n*’ = number of measurements.

6. Conclusions

The different orientations of the pervasive S2 foliation in the country rocks and magmatic foliation (Sm) in plutonic rocks suggests that the ductile deformation history of the country rocks predate the intrusion of the pluton. The only syn-intrusive ductile deformation of the country rocks is suggested by S2, which is asymptotic of the deeper margin of the pluton and affected by D7 folding (lower Pragnetta valley; see also Zanolini et al., 2007). The axial plane of D7 folding is subparallel to the magmatic foliation of the deeper part of the pluton (see to the Main Map or Zanolini et al., 2007). The country rocks of the deeper part of the pluton seem affected by syn-intrusive shear zones based on HT mylonitic foliation that wraps relict minerals, which are characteristic of HP conditions in HP metagranitoids. These structural relationships are consistent with the intrusion of the Biella pluton into the Sesia-Lanzo Zone in crustal conditions as shallow as or shallower than the greenschist facies conditions, which is consistent with the replacement of chlorite by contact metamorphic biotite (Figure 4(d)) and estimates of intrusion depth (Zanolini et al., 2010). The structural relationships between S2 and Sm in the shallower part of the pluton (Zanolini et al., 2010) suggest that the orientation of S2 may control the shape of the pluton margin by constituting a weak surface for country rocks to break, produce xenoliths (Figure 2(b)), and create room for magma intrusion (Figure 2(d)). Therefore, ‘forceful’ and ‘passive’ mechanisms may have acted during emplacement of the pluton at its deeper part and shallower part, respectively. The room provided by the country rocks may locally control the orientation of the magmatic foliation and flow during emplacement (i.e. both for ‘forceful’ and ‘passive’ intrusion in the Desate area and Tempietto area, respectively; see the Main Map). The minor crystal-plastic deformation that is recorded in monzonites may be attributed to the

later intrusion of the syenitic–granitic complex in to the monzonitic complex (Bigioggero et al., 1994). The syenitic to granitic aplitic dykes may represent melts from the syenitic–granitic complex that was emplaced in the previously cooled monzonitic complex. The brittle structures primarily postdate the pluton intrusion and may be related to the activity of the adjacent Canavese and Cremosina fault zones, with the exception of the thick cataclastic band between M. Mazzaro and Monte Tovo, which is interpreted as a thrust fault. Brittle structures that bear mineralisation, which may represent circulation paths of residual fluids, may be coeval with the late stages of magma crystallisation. The types of minerals that form pre-intrusive pervasive assemblages control the extent of the contact aureole. Indeed HP mineral assemblages render the rocks more susceptible to contact metamorphism compared with HT assemblages (see the Pragnetta Valley on the Main Map). The permeability to magmatic fluids, which is related to the abundance of oriented white mica crystals, may explain the varying degree of transformation of the metapelites and meta-aplites at the same distance from the pluton (refer to the Cima Cucco area). In addition, the greater the angle between the pervasive foliation of the country rocks and the pluton margin, the more magmatic fluid circulation and therefore aureole extent may be facilitated (compare the A. Pera and Oropa areas). This evidence is also consistent with the low efficiency and high efficiency of the thermal conductivity along the orthogonal and parallel directions, respectively, to [001] cleavage of white mica crystals (Fiorentini Potenza, 1969).

Note

1. After the main field seasons, a key outcrop just south of Ristor Rosazza was destroyed during construction of the road connecting Oropa and the Cervo valley. This outcrop has been left on the map to support and justify the interpretation of the boundary between syenite and monzonite.

Software

A geodatabase, including structural data, sample descriptions, photos, and outcrop contours, was created using Esri ArcGIS 10.0. The final map was drawn using Adobe Illustrator CS6. Polar projections of structures were plotted using StereoWinFull and polar density projections were plotted using Openstereo (Grohmann, Campanha, & Soares Junior, 2011).

Acknowledgements

The reviews by Alfons Berger and Antonio Funedda significantly improved the clarity of the text and map. The review by Chris Orton improved the map plate layout. M. Iole Spalla reviewed a previous version of the work. Guido Gosso, M. Iole Spalla, and Michele Zucali provided insightful suggestions during field and laboratory work. A. Rizzi assisted the SEM work. Mr Stellino facilitated use of the Alpe Pera shepherd hut and the Locanda Galleria Rosazza crew provided a friendly field base.

Disclosure statement

No potential conflict of interest was reported by the author.

Funding

This work was supported by the PRIN 2010–2011: ‘Nascita e morte dei bacini oceanici: processi geodinamici dal rifting alla collisione continentale negli orogeni mediterranei e circum-mediterranei’.

References

- Berger, A., Thomsen, T. B., Ovtcharova, M., Kapferer, N., & Micolli, I. (2012). Dating emplacement and evolution of the orogenic magmatism in the internal Western Alps: 1. The Miagliano Pluton. *Swiss Journal of Geosciences*, 105, 49–65.
- Bernardelli, P., Castelli, D., & Rossetti, P. (2000). Tourmaline-rich ore-bearing hydrothermal system of lower Valle del Cervo (Western Alps, Italy): Field relationships and petrology. *Schweizerische Mineralogische und Petrographische Mitteilungen*, 80, 257–277.
- Bigoggero, B., Colombo, A., Del Moro, A., Gregnanin, A., Macera, P., & Tunesi, A. (1994). The Oligocene Valle del Cervo Pluton: An example of shoshonitic magmatism in the Western Italian Alps. *Memorie di Scienze Geologiche, Padova*, 46, 409–421.
- Blenkinsop, T. (2000). *Deformation, microstructures and mechanisms in mineral and rocks*. New York: Kluwer Academic.
- Bussy, F., Venturini, G., Hunziker, J., & Martinotti, G. (1998). U-Pb ages of magmatic rocks of the western Austroalpine Dent-Blanche-Sesia Unit. *Schweizerische Mineralogische und Petrographische Mitteilungen*, 78, 163–168.
- Callegari, E., Cigolini, C., Medeot, O., & D'Antonio, M. (2004). Petrogenesis of calcalkaline and shoshonitic post-collisional Oligocene volcanics of the cover series of the Sesia Zone, Western Italian Alps. *Geodinamica Acta*, 17, 1–29.
- Carraro, F., & Ferrara, G. (1968). Alpine “tonalite” at Miagliano, Biella (Zona Dioritico-kinzigitica). *Schweizerische Mineralogische und Petrographische Mitteilungen*, 48, 75–80.
- Cenki-Tok, B., Oliot, E., Rubatto, D., Berger, A., Engi, M., Janots, E., . . . Goncalves, P. (2011). Preservation of Permian allanite within an Alpine eclogite facies shear zone at Mt Mucrone, Italy: Mechanical and chemical behavior of allanite during mylonitization. *Lithos*, 125, 40–50.
- Compagnoni, R., Dal Piaz, G. V., Hunziker, J. C., Gosso, G., Lombardo, B., & Williams, P. F. (1977). The Sesia-Lanzo Zone: A slice of continental crust, with alpine HP-LT assemblages in the Western Italian Alps. *Rendiconti della Società Italiana di Mineralogia e Petrologia*, 33, 281–334.
- Davies, J. H., & Von Blanckenburg, F. (1995). Slab breakoff: A model of lithosphere detachment and its test in the magmatism and deformation of collisional orogens. *Earth and Planetary Science Letters*, 129, 85–102.
- De Capitani, L., Fiorentini Potenza, M., Marchi, A., & Sella, M. (1979). Chemical and tectonic contributions to the age and petrology of the Canavese and Sesia-Lanzo ‘porphyrites’. *Atti Società Italiana di Scienze Naturali*, 120, 151–179.
- Delleani, F., Spalla, M. I., Castelli, D., & Gosso, G. (2012). Multiscale structural analysis in the subducted continental crust of the internal Sesia-Lanzo Zone (Monte Mucrone, Western Alps). In M. Zucali, M. I. Spalla, & G. Gosso (Eds.), *Multiscale structures and tectonic trajectories in active margins: Journal of the Virtual Explorer*, paper 7.
- Delleani, F., Spalla, M. I., Castelli, D., & Gosso, G. (2013). A new petro-structural map of the Monte Mucrone metagranitoids (Sesia-Lanzo Zone, Western Alps). *Journal of Maps*, 9, 410–424.
- Dolenec, T. (1994). Novi izotopski in radiometrični podatki o pohorskih magmatskih kamninah. *Rudarsko-metalurški zbornik*, 41, 147–152.
- Fiorentini Potenza, M. (1969). Movimento di elementi durante l'intrusione e metamorfismo di contatto del plutone della Valle del Cervo. *Rendiconti della Società Italiana di Mineralogia e Petrografia*, 25, 353–374.
- Fodor, L. I., Gerdes, A., Dunkl, I., Koroknai, B., Pécskay, Z., Trajanova, M., . . . Frisch, W. (2008). Miocene emplacement and rapid cooling of the Pohorje pluton at the Alpine-Pannonian-Dinaridic junction, Slovenia. *Swiss Journal of Geosciences*, 101, S255–S271.
- Giorgetti, G., Tropper, P., Essene, E. J., & Peacor, D. R. (2000). Characterization of non-equilibrium and equilibrium occurrences of paragonite/muscovite intergrowths in an eclogite from the Sesia-Lanzo Zone (Western Alps, Italy). *Contributions to Mineralogy and Petrology*, 138, 326–336.
- Grohmann, C. H., Campanha, G. A. C., & Soares Junior, A. V. (2011, May 15–19). *Openstereo: um programa livre e multiplataforma para análise de dados estruturais*. 13° Simpósio Nacional de Estudos Tectônicos, Campinas, SP, pp. 26–28.
- Handy, M. R., Babist, J., Wagner, R., Rosenberg, C. L., & Konrad, M. (2005). Decoupling and its relations to strain partitioning in continental lithosphere: Insight from the Periadriatic fault system (European Alps). In D. Gapais, J. P. Brun, & P. R. Cobbold (Eds.), *Deformation mechanism, rheology and tectonics: From minerals to lithosphere: Geological society* (pp. 249–276). London: Special Publications, Geological Society of London.

- Hobbs, B. E., Ord, A., Spalla, M. I., Gosso, G., & Zucali, M. (2010). The interaction of deformation and metamorphic reactions. In M. I. Spalla, A. M. Marotta, & G. Gosso (Eds.), *Advances in interpretation of geological processes: Refinement of multi-scale data and integration in numerical modelling* (pp. 189–222). London: Special Publications, Geological Society of London.
- Kapferer, N., Mercolli, I., Berger, A., Ovtcharova, M., & Fügenschuh, B. (2012). Dating emplacement and evolution of the orogenic magmatism in the internal Western Alps: 2. The Biella Volcanic Suite. *Swiss Journal of Geosciences*, *105*, 67–84.
- Koons, P. O. (1986). Relative geobarometry from high-pressure rocks of quartzofeldspathic composition from the Sesia Zone, Western Alps, Italy. *Contributions to Mineralogy and Petrology*, *93*, 322–334.
- Krummenacher, D., & Evernden, J. (1960). Détermination d'âge isotopique sur quelques roches des Alpes par la méthode K-Ar. *Schweizerische Mineralogische und Petrographische Mitteilungen*, *40*, 267–277.
- Lanza, R. (1977). Palaeomagnetic data from the andesitic and lamprophyric dykes of the Sesia-Lanzo Zone (Western Alps). *Schweizerische Mineralogische und Petrographische Mitteilungen*, *57*, 281–290.
- Lardeaux, J. M., & Spalla, M. I. (1991). From granulites to eclogites in the Sesia zone (Italian Western Alps): A record of the opening and closure of the Piedmont ocean. *Journal of Metamorphic Geology*, *9*, 35–59.
- Mayer, A., Cortiana, G., Dal Piaz, G. V., Deloule, E., De Pieri, R., & Jobstraibizer, P. (2003). U-Pb single ages of the Adamello batholith, Southern Alps. *Memorie di Scienze Geologiche Padova*, *55*, 151–167.
- Müller, W., Mancktelow, N. S., & Meier, M. (2000). Rb-Sr microchrons of synkinematic mica in mylonites: An example from the DAV fault of the Eastern Alps. *Earth and Planetary Science Letters*, *180*, 385–397.
- Oberli, F., Meier, M., Berger, A., Rosenberg, C. L., & Gieré, R. (2004). U-Th-Pb and $^{230}\text{Th}/^{238}\text{U}$ disequilibrium isotope systematics: Precise accessory mineral chronology and melt evolution tracing in the Alpine Bergell intrusion. *Geochimica et Cosmochimica Acta*, *68*, 2543–2560.
- Pagliani Peyronel, G. (1959). Il granito porfirico della media Valle del Cervo (Biella). *Rendiconti dell'Istituto Lombardo di Scienze e Lettere*, *93*, 379–398.
- Pamić, J., & Palincš, L. (2000). Petrology and geochemistry of Paleogene tonalites from the easternmost parts of the Periadriatic Zone. *Mineralogy and Petrology*, *70*, 121–141.
- Passchier, C. W., & Trouw, R. A. J. (2005). *Microtectonics*. Berlin: Springer.
- Passchier, C. W., Urai, J. L., Van Loon, J., & Willimas, P. F. (1981). Structural geology of the Central Sesia-Lanzo Zone. *Geologie en Mijnbouw*, *60*, 497–507.
- Paterson, S. R., Vernon, R. H., & Tobisch, O. T. (1989). A review of criteria for the identification of magmatic and tectonic foliation in granulites. *Journal of Structural Geology*, *11*, 349–363.
- Rebay, G., & Spalla, M. I. (2001). Emplacement at granulite facies conditions of the Sesia-Lanzo metagabbros: An early record of Permian rifting? *Lithos*, *58*, 85–104.
- Roda, M., Spalla, M. I., & Marotta, A. M. (2012). Integration of natural data within a numerical model of ablative subduction: A possible interpretation for the Alpine dynamics of the Austroalpine crust. *Journal of Metamorphic Geology*, *30*, 973–996.
- Romer, R. L., Schärer, U., & Steck, A. (1996). Alpine and pre-Alpine magmatism in the root-zone of the Western Central Alps. *Contributions to Mineralogy and Petrology*, *123*, 138–158.
- Romer, R. L., & Siegesmund, S. (2003). Why allanite may swindle about its true age. *Contributions to Mineralogy and Petrology*, *146*, 297–307.
- Rosenberg, C. L. (2004). Shear zones and magma ascent: A model based on a review of the tertiary magmatism in the Alps. *Tectonics*, *23*, 1–21.
- Rosenberg, C. L., & Handy, M. R. (2005). Experimental deformation of partially melted granite revisited; implication for the continental crust. *Journal of Metamorphic Geology*, *23*, 19–28.
- Rossetti, P., Agangi, A., Castelli, D., Padoan, M., & Ruffini, R. (2007). The Oligocene Biella Pluton (Italian Western Alps): New insight on the magmatic vs. hydrothermal activity in the Valsessera roof zone. *Periodico di Mineralogia*, *76*, 223–240.
- Rubatto, D., Gebauer, D., & Compagnoni, R. (1999). Dating of eclogite-facies zircons; the age of Alpine metamorphism in the Sesia-Lanzo Zone (Western Alps). *Earth and Planetary Science Letters*, *167*, 141–158.
- Rubatto, D., Regis, D., Hermann, J., Boston, K., Engi, M., Beltrando, M., & McAlpine, S. R. B. (2011). Yo-yo subduction recorded by accessory minerals in the Italian Western Alps. *Nature Geoscience*, *4*, 338–342. doi:10.1038/ngeo1124.
- Rubbo, M., Borghi, A., & Compagnoni, R. (1999). Thermodynamic analysis of garnet growth zoning in eclogite facies granodiorite from M. Mucrone, Sesia Zone, western Italian Alps. *Contributions to Mineralogy and Petrology*, *137*, 289–303.

- Spalla, M. I., Zanoni, D., Marotta, A. M., Rebay, G., Roda, M., Zucali, M., & Gosso, G. (2014). The transition from Variscan collision to continental break-up in the Alps: Insights from the comparison between natural data and numerical model predictions. In K. Schulmann, J. R. Martínez Catalán, J.-M. Lardeaux, V. Janoušek, & G. Oggiano (Eds.), *The Variscan orogeny: Extent, timescale and the formation of the European crust*. London: Special Publications, Geological Society of London. doi:10.1144/SP405.11.
- Spalla, M. I., Zucali, M., di Paola, S., & Gosso, G. (2005). A critical assessment of the tectono-thermal memory of rocks and definition of the tectono-metamorphic units: Evidence from fabric and degree of metamorphic transformations. In D. Gapais, J. P. Brun, & P. R. Cobbold (Eds.), *Deformation mechanisms, rheology and tectonics: From minerals to the lithosphere* (pp. 227–247). London: Special Publications, Geological Society of London.
- Spalla, M. I., & Zulbati, F. (2003). Structural and petrographic map of the Southern Sesia-Lanzo Zone (Monte Soglio – Rocca Canavese, Western Alps, Italy). *Memorie di Scienze Geologiche Padova*, 55, 119–127.
- Stipp, M., Fügenschuh, B., Gromet, L. P., Stünitz, H., & Schmid, S. M. (2004). Contemporaneous plutonism and strike-slip faulting along the easternmost segment of the Insubric line: The Tonale fault zone north of the Adamello pluton (Italian Alps). *Tectonics*, 23, TC3004.
- Tobisch, O. T., & Williams, Q. (1997). Use of microgranitoid enclaves as solid state strain markers in deformed granitic rock: An evaluation. *Journal of Structural Geology*, 20, 727–743.
- Tropper, P., & Essene, E. J. (2002). Thermobarometry in eclogites with multiple stages of mineral growth: an example from the Sesia-Lanzo Zone (Western Alps, Italy). *Schweizerische Mineralogische und Petrographische Mitteilungen*, 82, 487–514.
- Tropper, P., Essene, E. J., Sharp, Z. D., & Hunziker, J. C. (1999). Application of K-feldspar-jadeite-quartz barometry to eclogite facies metagranites and metapelites in the Sesia Lanzo Zone (Western Alps, Italy). *Journal of Metamorphic Geology*, 17, 195–209.
- Van Merke de Lummen, G., & Vander Auwera, J. (1990). Petrogenesis of Traversella diorite (Piemonte Italy): A major trace element and isotopic (O, Sr) model. *Lithos*, 24, 121–136.
- Vernon, R. H. (2004). *A practical guide to rock microstructure*. Cambridge: Cambridge University Press.
- Von Blanckenburg, F., & Davies, J. H. (1995). Slab breakoff. A model for syncollisional magmatism and tectonics in the Alps. *Tectonics*, 14, 120–131.
- Von Blanckenburg, F., Früh-Green, G., Diethelm, K., & Stille, P. (1992). Nd-, Sr-, O-isotopic and chemical evidence for a two-stage contamination history of mantle magma in the Central-Alpine Bergell intrusion. *Contributions to Mineralogy and Petrology*, 110, 33–45.
- Von Blanckenburg, F., Kagami, H., Deutsch, A., Oberli, F., Meier, M., Wiedenbeck, M., ... Fischer, H. (1998). The origin of Alpine plutons along the Periadriatic Lineament. *Schweizerische Mineralogische und Petrographische Mitteilungen*, 78, 55–65.
- Whitney, D. L., & Evans, B. W. (2010). Abbreviations for names of rock-forming minerals. *American Mineralogist*, 95, 185–187.
- Williams, P. F. (1985). Multiply deformed terrains – problems of correlation. *Journal of Structural Geology*, 7, 269–280.
- Zanoni, D. (2007). *Messa in posto di plutoni tardo collisionali in unità continentali profonde esumate. L'esempio della Zona Sesia Lanzo (Alpi Occidentali Interne)* (Unpublished Ph.D. thesis) (320 pp.). Università di Milano.
- Zanoni, D. (2010). Structural and petrographic analysis at the north-eastern margin of the Oligocene Traversella pluton (Internal Western Alps, Italy). *Bollettino della Società Geologica Italiana* [Italian Journal of Geoscience], 129, 51–68.
- Zanoni, D., Bado, L., Spalla, M. I., Zucali, M., & Gosso, G. (2008). Structural analysis of the Northeastern margin of the tertiary intrusive stock of Biella (Western Alps, Italy). *Bollettino della Società Geologica Italiana* [Italian Journal of Geoscience], 127, 125–140.
- Zanoni, D., Spalla, M. I., & Gosso, G. (2010). Structure and PT estimates across late-collisional plutons: Constraints on the exhumation of western Alpine continental HP units. *International Geology Review*, 52, 1244–1267.
- Zanoni, D., Spalla, M. I., Gosso, G., & Zucali, M. (2007). Emplacement of late-collisional plutons in exhumed deep crustal slices: The case of the Sesia Lanzo Zone (Internal Western Alps). *Rendiconti della Società Geologica Italiana*, 5, 228–230.
- Zucali, M. (2002). Foliation map of the “Eclogitic Micascists Complex” (Monte Mucreone – Monte Mars – Mombarone, Sesia-Lanzo Zone, Italy). *Memorie di Scienze Geologiche, Padova*, 54, 87–100.

- Zucali, M., & Spalla, M. I. (2011). Prograde lawsonite during the flow of continental crust in the Alpine subduction: Strain vs. metamorphism partitioning, a field-analysis approach to infer tectonometamorphic evolutions (Sesia-Lanzo Zone, Western Italian Alps). *Journal of Structural Geology*, 33, 381–398.
- Zucali, M., Spalla, M. I., & Gosso, G. (2002). Strain partitioning and fabric evolution as a correlation tool: The example of the eclogitic micaschists complex in the Sesia-Lanzo Zone (Monte Mucrone – Monte Mars, Western Alps Italy). *Schweizerische Mineralogische und Petrographische Mitteilungen*, 82, 429–454.